ELSEVIER

Earth and Planetary Science Letters 199 (2002) 49–65

EPSL

www.elsevier.com/locate/epsl

HFSE residence and Nb/Ta ratios in metasomatised, rutile-bearing mantle peridotites

F. Kalfoun [a], D. Ionov [b,*], C. Merlet [a]

[a] *ISTEEM, CC 049, CNRS, Université de Montpellier II, pl. E. Bataillon, 34095 Montpellier Cedex 5, France*

[b] *Département des Sciences de la Terre et de l'Environnement, P.O. Box 160/02, Université Libre de Bruxelles, 50 av. F.D. Roosevelt, B-1050 Brussels, Belgium*

Received 25 June 2001; received in revised form 22 February 2002; accepted 22 February 2002

Abstract

We have constrained the residence of high field strength elements (Nb, Ta, Zr, Hf, Ti) in metasomatised peridotite xenoliths in basalts from SE Siberia using high-precision electron-microprobe analyses of accessory Ti-rich oxides and solution inductively coupled plasma mass spectrometry analyses of whole rocks and clinopyroxene. Highest Nb abundances (0.9–4.5%) were found in rutile, compared with $<0.5\%$ in armalcolite and loveringite and $<0.1\%$ in ilmenite. Mass-balance calculations indicate that only 1–5% of Nb and Ta in the rocks reside in major minerals and that the rest may be hosted by the Ti-oxides. The Nb/Ta values in the Ti-oxides ($\pm$ 2–5% accuracy at Ta $\geq$ 1000 ppm) range significantly between individual grains in each sample (e.g. 11–37) but their averages are close to Nb/Ta in the bulk rock. Thus, the whole-rock Nb/Ta can be constrained from analyses of the Nb-rich phases. High ZrO_2 (1–7%) was found in loveringite and rutile. However, these minerals alone do not control whole-rock Zr/Hf in the peridotites because, unlike the Nb–Ta pair, much of Zr and Hf also resides in pyroxenes. Loveringite typically has high La and Ce (up to 1.6 wt%) and may be an important light rare earth element host. Overall, the Ti-oxide micro-phases may be essential components in nondescript grain boundary materials that are believed to host much of the highly incompatible elements in some mantle rocks and play a role in the behaviour of those elements during melting and metasomatism. Whole-rock Nb/Ta values in most of the peridotites are higher than the chondritic ratio (17.5). A literature review finds largely chondritic and subchondritic Nb/Ta and Zr/Hf in abyssal and massif peridotites, consistent with an origin as partial melting residues (based on peridotite/melt partition coefficients). By contrast, superchondritic Nb/Ta, as well as high La/Yb, is common in mantle xenoliths, indicating that metasomatism may increase Nb/Ta, together with La/Yb, in the initially depleted peridotites. If the high Nb/Ta predominates in the lithospheric mantle (assuming most of it has been metasomatised), it may provide a reservoir complementary to those of asthenospheric mid-ocean ridge basalt-type mantle and continental crust, which both have subchondritic Nb/Ta. However, the lithospheric mantle is not likely to counterbalance the subchondritic reservoirs in the bulk earth, firstly, because of a much higher mass of the asthenospheric mantle and higher Nb and Ta in the crust, and secondly, because many metasomatised peridotites (including all samples in this study) have subchondritic Nb/La.

Keywords: niobium; tantalum; peridotites; mantle; metasomatism

* Corresponding author. Tel.: +32-2-650-2219; Fax: +32-2-650-3748. *E-mail address:* dionov@ulb.ac.be (D. Ionov).

0012-821X/02/$ – see front matter
PII: S0012-821X(02)00555-1

1. Introduction

Nb, Ta and other high field strength elements (HFSE) are widely used as geochemical indicators of geological processes and in global earth models. In particular, the depletion of Nb and Ta relative to light rare earth elements (REE) and other highly incompatible elements is characteristic of the continental crust and island-arc basalts but is not observed in mid-ocean ridge basalts (MORB) and oceanic island basalts (e.g. [1–3]). The Nb–Ta and Zr–Hf pairs were long thought to be geochemically inseparable (because of matching valence state and atomic radii), and their ratios assumed nearly constant.

Advances in analytical techniques have highlighted a seeming paradox in the bulk earth balance of Nb and Ta. Those two elements are refractory and lithophile, and therefore Nb/Ta in the bulk silicate earth should be similar to chondritic (17.5 ± 0.6) [4]. Recent studies have shown that two global terrestrial reservoirs, the continental crust and the depleted mantle (DM, source of MORB), which are thought to be complementary, both have subchondritic Nb/Ta values of 12 (crust) [5,6] and 15.5 (MORB) [7]. That finding has given a new impetus to the search for a 'hidden' superchondritic reservoir capable of balancing the subchondritic reservoirs [3,8,9]. It also further emphasised the importance of research into possible origins for variations in Nb/Ta [10,11]. For the Zr–Hf pair, significant variations in Zr/Hf were found in oceanic basalts and related to metasomatic processes in their mantle sources [12].

Nb and Ta inventory of the lithospheric mantle, another global reservoir apart from the crust and asthenospheric (depleted) mantle, is not well defined. A major difficulty is posed by low abundances of Nb and particularly Ta in common mantle rocks that may hinder precise determination of their Nb/Ta. One way to address that problem is by studies of minerals that concentrate Nb and Ta. Ionov and Hofmann [13] and Ionov et al. [14] suggested that amphibole and phlogopite control the Nb–Ta budget in 'hydrous' mantle rocks. Studies of 'anhydrous' mantle peridotites have shown that only a small fraction of the whole-rock inventory of Nb and Ta is hosted by olivine, pyroxenes and spinel [15,16]. It was suggested that many highly incompatible elements reside in the interstitial material of the peridotites and in particular that Nb and Ta may be hosted by titanium-rich oxide micro-phases [17]. Rutile is a common accessory phase in eclogites [18] and is occasionally present in metasomatised peridotites. It may contain as much as 4–6% of Nb_2O_5 [19] and, because it highly concentrates Nb and Ta, the relative abundance of Nb and Ta in that mineral may largely control that of the bulk rock [9]. Rutile is believed to be very rare in off-cratonic mantle rocks [20]. When present, its grains are too small (< 20 μm) to be separated or analysed in situ by laser ablation microprobe inductively coupled plasma mass spectrometry (LAM-ICPMS) and in many cases even by electron microprobe [17].

In this study we develop a high-precision electron probe microbeam analysis (EPMA) technique to determine trace elements and obtain Nb/Ta and Zr/Hf values with precision of ± 2–6% in rutile and other Ti-rich oxides in peridotite xenoliths. These data, together with solution ICPMS analyses of clinopyroxene (cpx) and bulk rock peridotites, enable the definition of the residence and mass balance of HFSE and other trace elements in the xenoliths and are also relevant to other mantle rocks. Finally, we compare HFSE abundances and Nb/Ta and Zr/Hf values in depleted and metasomatised peridotites and examine the Nb–Ta budget of the lithospheric mantle.

2. Analytical techniques

EPMA data were obtained on a CAMECA SX-100 electron microprobe equipped with five wavelength-dispersive X-ray spectrometers (WDS). The small size of the Ti-rich oxides limits possibilities of using high accelerating voltage and high beam current required to measure elements at low abundances with EPMA [21]. Those constraints require a compromise between peak-counting statistics, background, beam drift, stray radiation and contamination that was sought in this work

Table 1
Concentrations of Nb, Ta, Zr and Hf, and Nb/Ta and Zr/Hf values in Ti-oxide minerals from high-precision EPMA

Grain No.	Mineral	Ta		Hf		Nb		Zr		Nb/Ta		Zr/Hf	
		wt%	2σ	wt%	2σ	wt%	2σ	wt%	2σ		2σ		2 σ
9513-7-SW2d	rutile	0.120	1.7	0.023	19	2.17	1.3	0.86	1.2	18.1	2.1	38.2	19.3
9513-7-NWb	rutile	0.050	3.9	0.043	10	0.918	1.7	2.37	1.1	18.3	4.3	54.8	10.4
9513-7-NWg	rutile	0.032	6.1	0.037	12	0.911	1.7	1.84	1.1	28.6	6.3	50.1	12.1
9513-7-NWa	rutile	0.033	5.8	0.041	11	1.09	1.7	2.07	1.1	32.7	6.0	50.3	10.8
9513-7-NWf	rutile	0.058	3.4	0.026	17	0.965	1.6	1.12	1.1	16.8	3.8	42.2	16.6
Mean		0.059		0.034		1.21		1.65		22.9		47.1	
Abundance-weighed average										22.1		49.2	
9513-13-14a	loveringite	0.025	11	0.038	12	0.282	3.2	2.21	1.1	11.3	11.5	58.1	11.6
9513-13-20a	armalcolite	0.022	10	0.025	13	0.433	2.4	0.88	1.2	19.7	10.3	35.3	13.1
9513-13-14k	rutile	0.122	2	0.064	8	4.48	1.1	2.98	1.1	36.7	2.3	46.6	7.6
9513-13-17a	rutile	0.102	2	0.040	11	2.19	1.3	1.60	1.1	21.5	2.4	40.1	11.3
9513-13-20c	rutile	0.088	3	0.063	7	2.4	1.3	2.92	1.1	27.3	3.3	46.3	7.3
9513-13-18g	rutile	0.116	2	0.044	11	1.37	1.5	2.11	1.1	11.8	2.5	48.0	10.7
9513-13-16a	rutile	0.113	2	0.026	18	1.89	1.3	1.11	1.2	16.8	2.4	42.8	17.7
Mean		0.084		0.043		1.86		1.97		20.7		45.3	
Abundance-weighed average										25.8 (20.1)		46.8	

using recent developments in microanalysis such as spectrum simulation and X-ray emission modeling. The EPMA procedure is described in full elsewhere (Kalfoun et al., in press) and its summary is provided in the Appendix of the **Background Data Set**[1]. The overall precision of individual Nb/Ta values is ±3–14% (2σ) at Ta ≥ 200 ppm and ±2–3% at Ta ≥ 1000 ppm. The abundances and ratios of Nb, Ta, Zr and Hf obtained with this procedure are presented in Table 1, along with precision estimates from repeated analyses.

ICPMS analyses were done on a Fisons (VG-Elemental) PQ2+Turbo (PlasmaQuad II+®) instrument. The analytical method is similar to that described by Ionov et al. [22]. Hand-picked cpx separates were leached in 20% HF and 25% HNO_3 prior to dissolution to remove contamination on surface and in cracks. Whole-rock powders (~100 mg) and mineral separates (10–20 mg) were dissolved in HF–$HClO_4$ mixture followed by repeated evaporation with $HClO_4$ and with 2 ml of 6 N HNO_3. Dried samples were taken up in HNO_3 and diluted to 1:1000 (in 2% HNO_3) shortly before the analysis. 2% HNO_3 was used for rinsing (3 min) between each measurement. In and Bi were used as internal standards for drift correction. Two series of composite synthetic external standards that enable corrections for oxide interference were used for calibration. Two chemical blanks and two or three international reference materials were run with each sample batch. Typical blank values for Nb, Ta, Zr and Hf (in ppb) are 0.4, 0.2, 1.5 and 0.47, respectively [23]. The overall precision (2σ) of the Nb/Ta and Zr/Hf values in the whole-rock peridotites and reference samples is 6–8%. Further details are given in the Appendix of the **Background Data Set**[1].

3. Sample description

The search for accessory minerals rich in Nb and Ta and appropriate for EPMA was carried out in several off-cratonic mantle peridotite suites in which they were previously reported. In most of them [17,24], rutile and other Ti-oxide phases were too small for high-precision EPMA. This study was done on spinel lherzolite xenoliths from Barhatny, a late Cenozoic basaltic eruption

[1] http://www.elsevier.com/locate/epsl

centre in northern Sikhote-Alin (SE Siberia, Russia). Some of them contain arguably the largest and most abundant Ti-rich oxides reported so far from off-cratonic mantle [20]. The sample selection was guided by results of an earlier petrographic and geochemical study of a larger collection from that locality [25], which also provided some modal and major element data. The present work is focussed on the budget and ratios of Nb, Ta, Zr, Hf and some other trace elements in selected xenoliths and is largely based on original high-precision EPM and solution ICPMS analyses of their minerals and whole rocks.

The Barhatny lherzolites have moderate to high modal cpx and range from LREE-depleted to LREE-enriched [20]. At least half of the xenoliths contain pockets and cross-cutting veins made up of fine-grained feldspar, Ti-rich oxides and second-generation olivine, cpx and Cr-spinel (Fig. 1). The metasomatic aggregates replace primary spinel and orthopyroxene (and also accessory amphibole and mica, if present) [20]. No silicate glass was found in any of the xenoliths. Four peridotites with the most abundant and largest Ti-oxides (and high modal feldspar, 2–3%) were selected for this study. For comparison, we have also done ICPMS analyses of four whole-rock xenoliths that contain no or very little feldspar or Ti-oxides (three cpx-rich and one cpx-poor lherzolites).

Minerals in fine-grained metasomatic pockets in sample 9513-7 (Fig. 1b) were analysed by EPM for major elements (Table 1 of the **Background**

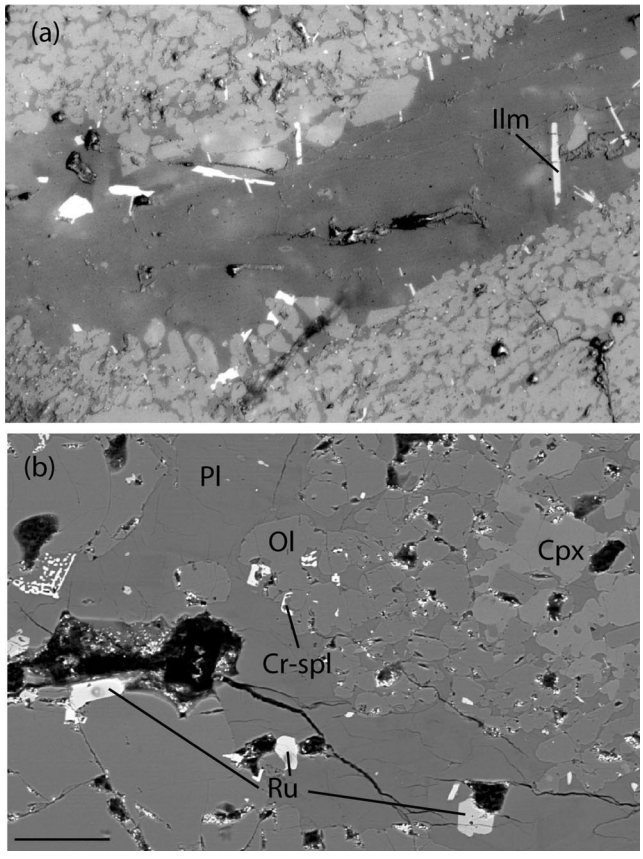

Fig. 1. (a) Photomicrograph of a feldspar-rich vein in spinel lherzolite 9513-13 (reflected light, view field is 2.5 mm). Note accessory Ti-rich oxides (bright) and metasomatic alteration around the vein. (b) BSE image of an interstitial feldspar-rich pocket (dark grey) and associated second-generation cpx, olivine (Ol) and Cr-spinel in sample 9513-7. Note circular marks left on rutile (Ru) grains by EPMA beam. Scale bar is 50 μm. Pl = feldspar, Ilm = ilmenite.

Data Set[1]). Compared with minerals in the host peridotite, olivine has higher Fe and Ca; spinel has lower Cr/(Cr+Al). Cpx is low in Al_2O_3 (0.6–1.8%) and Na_2O (0.4–0.7%), consistent with equilibration with feldspar. Feldspar contains 4–7% Na_2O and has a broad range of K_2O (0.3–10%) and CaO (0.02–10%), similar to other metasomatised Barhatny xenoliths ([20] and unpublished data of D. Ionov).

4. Mineralogy and composition of Ti-rich oxides

4.1. Textural position and mineral species

The Ti-rich oxides vary greatly in shape and size. Randomly oriented needle-, rod- and blade-like grains are common in feldspar-rich veins; they are usually $\leq$10–20 μm in thickness, but may be $>$100 μm in length (Fig. 1a). Ti-oxides in interstitial pockets tend to be smaller and anhedral (Fig. 1b). Back-scattered electron (BSE) and X-ray images show that many of the grains are composite and may have a complex structure displaying a core and a rim with distinct compositions, a matrix with exsolution lamellae or both (Fig. 2). The matrix commonly has rutile composition whereas rims and lamellae are made up of ilmenite. The rims and lamellae are usually too thin for quantitative trace element analysis. Nevertheless, X-ray images clearly demonstrate that the rutile is rich in Nb and Zr, whereas the contents of those elements in the ilmenite are much lower (Fig. 2).

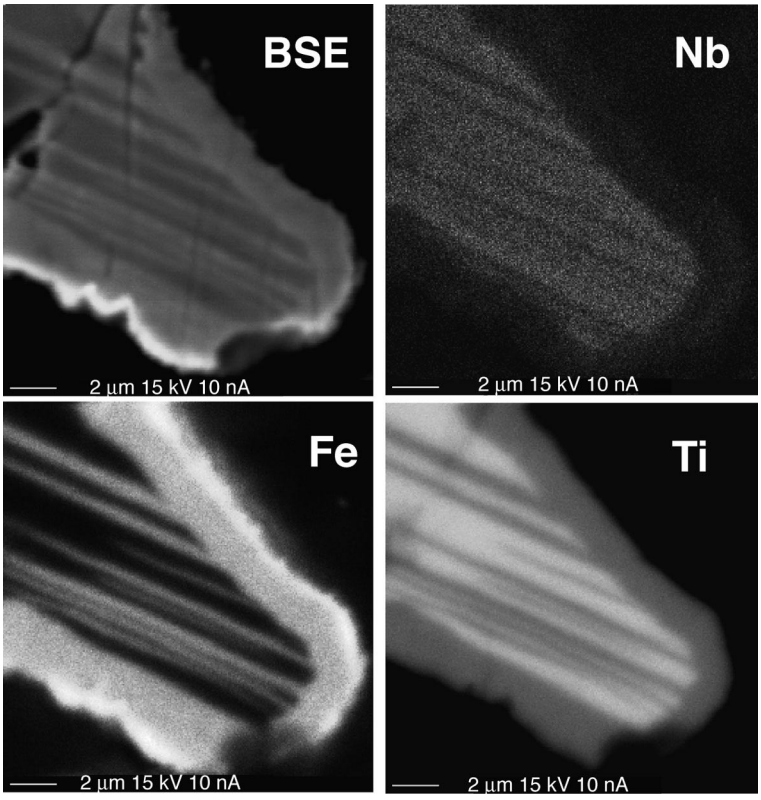

Fig. 2. BSE and X-ray (Fe, Ti and Nb) images of a composite Ti-rich oxide grain in sample 9513-7 (scale bar is 2 μm). Rutile (high Ti, low Fe) makes up the core of the grain, which contains exsolution lamellae and is rimmed with ilmenite (?). Rutile has higher Nb, Ta, Zr and Hf than ilmenite (?).

Composite Ti-oxide inclusions were earlier reported from pyrope xenocrysts from SW USA [26]. Ilmenite exsolution (on a scale of 10–100 μm) was routinely found by optical studies in cratonic kimberlite-borne rutiles (e.g. [19]). However, micrometer-scale heterogeneity in Ti-oxide minerals revealed in this study by X-ray imaging has not been previously reported, at least for off-cratonic mantle xenoliths. Because its scale is close to the size of electron beam, EPMA data obtained without appropriate prior homogeneity checks may represent mixtures of phases and should be treated with caution. The spread in major and trace element compositions of off-cratonic Ti-oxide minerals reported previously [20,27] may be partly due to analysis of heterogeneous materials, with electron beam overlapping different phases.

Representative analyses of Ti-rich oxide minerals are provided in Table 2 of the **Background Data Set**[1]. The chemical compositions outline at least four distinct mineral species or series: ilmenite, rutile, armalcolite and chrichtonite (Ca-Cr armalcolite) (Fig. 3a). Ilmenite is the most common Ti-rich phase followed by rutile; the other minerals are rare and usually smaller in size. Optical identification of individual grains by their shape or reflectivity is extremely difficult; they were normally recognised by X-ray scanning followed by EPMA. Some values for minor components in Table 2 of the **Background Data Set**[1] should be treated with caution because of potential problems with analyzing small grains, in particular stray radiation from the host. Those problems were monitored and dealt with during precise analyses for Ti, Si, Nb, Ta, Zr and Hf (Table 1), but not in routine analyses. For instance, the values for Al, Mg and Ca in rutile and for Al and Ca in ilmenite are probably below detection limits in most grains.

4.2. Major and trace element compositions

The majority of analyses in Table 1 are for rutile because that mineral was found to be richest in Nb and therefore of most interest for Nb/Ta determination. Nb_2O_5 in rutile ranges from 1.2 to 5.6% while ZrO_2 ranges from 1 to 4% (Fig. 3b), similar to results obtained earlier by Ionov et al.

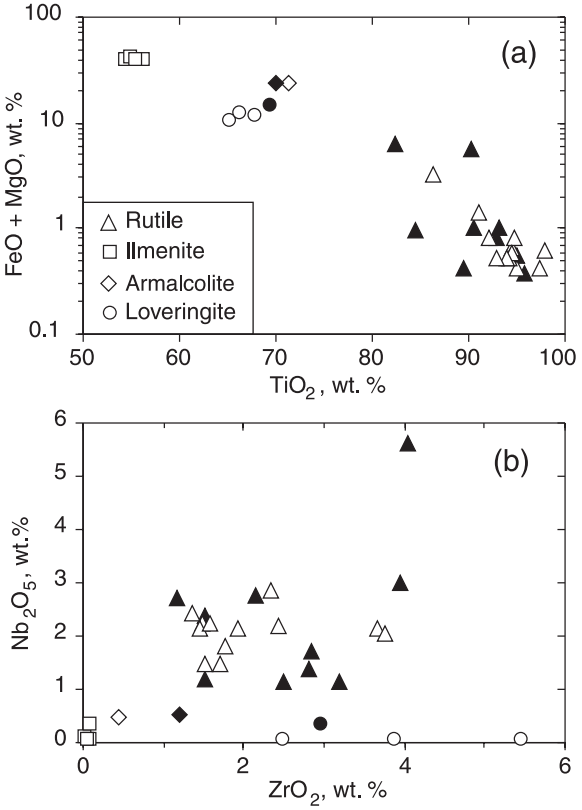

Fig. 3. TiO_2 vs. MgO+ΣFeO (a) and ZrO_2 vs. Nb_2O_5 (b) for Ti-rich oxide minerals. Filled symbols are grains used for high-precision EPMA for Nb, Ta, Zr and Hf.

[20]. Mean Zr/Nb ratio in 11 rutile grains is close to unity (0.95, range 0.4–2.6), indicating that Zr and Nb enter rutile in nearly equal amounts, probably constrained by isomorphic substitution mechanisms. The Barhatny rutiles have higher maximal Nb and Zr than those reported for metasomatised peridotite xenoliths from South African kimberlites [19], Tanzania [9], Kerguelen [27] and pyrope xenocrysts from SW USA [26]. Higher Nb was previously reported only for rutile from some rare xenolith types from Jagersfontein [19]. The majority of rutile grains (see Table 2 of the **Background Data Set**[1]) contain significant Cr_2O_3 (up to 3%) and ΣFeO (up to 5.2%), which are common for rutile of mantle origin and may play a role in HFSE substitution into TiO_2 lattice (e.g. [19]). By contrast, we found no Al-bearing rutiles reported earlier from experimental work [28]. Ru-

Table 2
EPM analyses of chrichtonite series minerals (wt%)

	9513-13					9513-7
	14e-1	14e-2	15b	15c	17f	SW2C
SiO_2	0.68	0.49	0.44	0.26	0.27	0.26
TiO_2	61.2	63.9	66.1	66.3	62.8	61.0
Al_2O_3	0.59	0.62	0.73	0.72	0.86	0.48
Cr_2O_3	6.63	4.13	12.3	12.1	14.3	12.8
FeO	10.7	11.9	9.66	8.84	7.71	9.61
MgO	3.51	3.88	3.48	3.49	3.58	3.40
CaO	2.17	2.05	3.07	3.07	2.67	1.92
ZrO_2	6.16	7.01	2.58	4.77	5.55	4.27
Nb_2O_3	0.06	0.04	0.04	0.08	0.03	0.01
La_2O_3	0.97	1.35	0.69	0.24	0.28	1.30
Ce_2O_3	1.23	1.40	0.96	0.46	0.54	1.92
Y_2O_3	0.11	0.09	0.06	0.05	0.07	0.11
Total	94.0	96.9	100.1	100.3	98.6	97.1

tile analysis with highest Fe (9513-7sw2dark) has low TiO_2 (82%) and a low total (95%); it was done on a composite grain (Fig. 2) apparently produced by exsolution. Ilmenite has significant Cr_2O_3 (1–2%), but is low in Nb and Zr and therefore unsuitable for determination of Nb/Ta and Zr/Hf.

Armalcolite is a pseudobrookite group mineral commonly defined as $(Mg,Fe)Ti_2O_5$ (e.g. [19]). Armalcolite from Barhatny contains 70–72% TiO_2, 1–2% Al_2O_3, 1–3% Cr_2O_3, and has high MgO (10.8–12.5%) compared to the majority of cratonic armalcolites. Its composition fits well with a normal pseudobrookite formula, whereas some other minerals also included in that group [29] have a wider range in (Mg,Fe)/Ti. The abundances of Nb and Zr in armalcolite are much lower than in rutile (Table 1, Fig. 3b).

Loveringite is a Ca-rich end-member of the chrichtonite series that has a general formula $AM_{21}O_{38}$, where A is a large-radius cation (Ca, Na, Sr, REE, etc.) and M are smaller cations (Ti, Mg, Fe, Cr, Al, Zr) ([19,26] and references therein). Minerals with similar compositions have also been described as Ca-Cr-(Zr)-armalcolites [19,20,27]. We prefer to identify the Ca-bearing Ti-rich minerals from Barhatny as chrichtonites because their cation ratios are in fair agreement with the loveringite formula but do not fit well with armalcolite or magnetoplumbite ($AM_{12}O_{19}$), and because getting Ca (and REE, see below) into pseudobrookite appears quite problematic. These fine-grained minerals are normally too small for X-ray structure determinations, but recently Wang et al. [26] obtained a diffraction pattern matching that of chrichtonite on an inclusion from pyrope with a composition similar to those reported here.

Loveringite differs from armalcolite by the presence of CaO (1.9–3.2%) and distinctly lower MgO (3–4%). In addition, it has variable but typically much higher Cr_2O_3 (2.4–14.3%) and somewhat lower TiO_2 (61–69%) than armalcolite (Fig. 3a), and may also contain Na, K and REE (Table 2). Furthermore, it is consistently low in Nb_2O_5 (0.2%), but has the highest ZrO_2 (2.6–7.0%) among the Barhatny Ti-rich oxide minerals (Fig. 3b). The abundances of Cr, Fe and Zr are negatively correlated to each other, but do not appear to be correlated with Ti (Fig. 4), indicating limited isomorphic substitution at the M-site.

High-precision analyses of loveringite for REE (Table 2) have yielded significant La_2O_3 and Ce_2O_3 (0.3–2%) and much lower Y_2O_3 (0.05–0.12%), whereas no heavy or medium REE have been detected. Atomic radius of Y is close to that of Ho and Er, and because Y abundance deduced for the primitive mantle is much higher than those of La and Ce [1] we conclude that the loveringite is strongly enriched in light over medium and

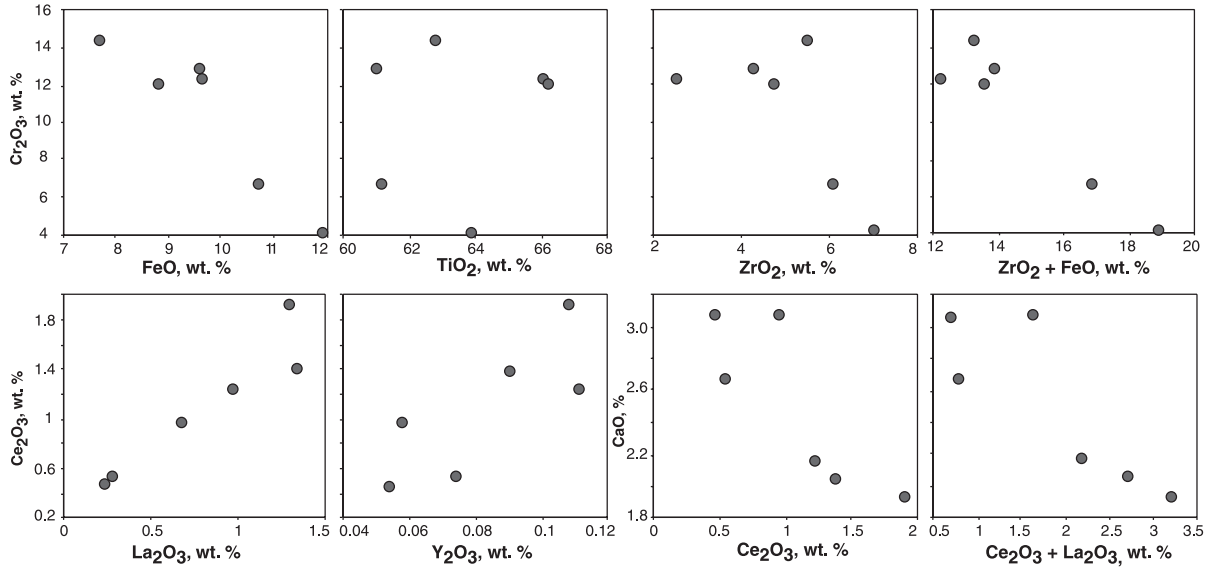

Fig. 4. Oxide co-variation diagrams for Ca-REE chrichtonite series minerals.

heavy REE. The abundances of La, Ce and Y are positively correlated to each other, but show a negative correlation with CaO (Fig. 4). The latter is consistent with isomorphic substitution at the chrichtonite A-site and indicates that the REE-rich compositions are intermediate between the Ca (loveringite) and REE (davidite) end-member minerals of the chrichtonite series [30].

4.3. Nb/Ta and Zr/Hf in the Ti-rich oxide minerals

Nb/Ta and Zr/Hf values calculated from high-precision EPMA are given in Table 1. Nb/Ta in rutile ranges from 17 to 33 in sample 9513-7 and from 11 to 37 in 9513-13 thus showing significant variation between mineral grains in each sample (Fig. 5). Zr/Hf ranges from 38 to 55 in 9513-7 and from 40 to 48 in 9513-13. One loveringite and one armalcolite analysed in 9513-13 have Nb/Ta within the range found in rutile, but show the highest and lowest Zr/Hf values, respectively (58 and 35), in that sample.

Mean Nb/Ta for five analyses in sample 9513-7 (22.9) and seven analyses in 9513-13 (20.7) are not very different; the mean Zr/Hf values are similar as well (47.1 and 45.3). More correct (in terms of impact on bulk rock values) average estimates may be obtained by weighting values for each grain using its mass and abundances of Nb and Zr. Grain mass, however, is hard to estimate as it may not be proportional to random surface exposure areas. Weighting the averages by Zr abundances yields somewhat higher Zr/Hf (49.2 and 46.8) because Zr-rich grains have slightly higher Zr/Hf. Weighting average Nb/Ta by Nb yields a lower value (22.1) for 9513-7 and a higher value (25.8) for 9513-13. The latter, however, is due to very high Nb/Ta in a single Nb-rich grain (Fig. 5).

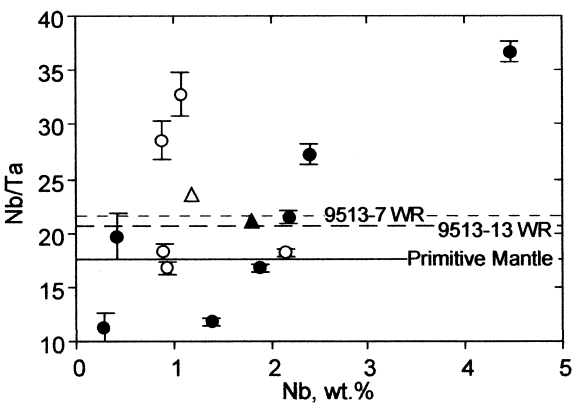

Fig. 5. Nb/Ta in Ti-rich oxide minerals (with error bars) and in whole-rock peridotites. Empty symbols, EPMA of minerals and their mean for 9513-7; filled symbols, same for 9513-13.

Table 3
Solution ICPMS analyses of whole-rock samples and mineral separates (ppm)

	9513-7		9513-8		9513-13		9513-36			9513-2	9513-4	9513-34	9512-5	UB-N reference sample		
	WR	Cpx	WR	Cpx	WR	Cpx	WR	Cpx	Fs+Ox	WR	WR	WR	WR	Mean ($n=3$)	S.D. (2σ)	R.V.
Rb	2.61	0.52	6.14	6.32	3.36	0.19	3.30	0.13	7.12	0.30	0.19	0.31	0.52	3.11	0.01	4
Sr	59.8	354	58.0	275	54.2	184	83	371	380	9.4	7.6	16.1	9.1	6.85	0.32	9
Zr	3.26	9.5	7.2	29.0	12.6	27.1	4.65	38.1	24.8	4.51	3.90	8.27	4.12	3.60	0.30	4
Nb	0.84	0.208	1.57	0.90	2.71	1.06	0.52	0.039	3.42	0.145	0.105	0.205	0.366	0.053	0.002	0.05
Cs	0.014	-	0.031	0.011	0.022	0.01	0.0094	0.001	0.013	0.006	0.006	0.002	0.0093	10.3	0.4	10
Ba	25.1	10.9	38.9	51.1	36.6	2.66	44.4	11.2	255	2.9	2.4	3.6	1.9	25.9	0.2	27
La	5.88	32.8	5.71	23.7	3.61	10.4	6.26	28.1	19.2	0.33	0.21	0.69	0.69	0.32	0.02	0.35
Ce	9.8	60.4	10.7	48.2	7.2	19.0	8.3	25.9	28.7	0.62	0.40	1.29	1.42	0.78	0.03	0.80
Pr	0.80	4.53	1.10	4.56	0.84	2.15	0.71	1.59	2.63	0.11	0.081	0.201	0.169	0.11	0.01	0.12
Nd	2.25	12.1	3.84	14.7	3.33	9.09	2.23	5.14	9.0	0.57	0.45	1.02	0.68	0.60	0.02	0.60
Sm	0.24	1.24	0.57	2.00	0.65	2.09	0.35	1.48	1.40	0.19	0.160	0.313	0.120	0.21	0.01	0.20
Eu	0.08	0.47	0.20	0.70	0.24	0.83	0.13	0.61	0.52	0.078	0.066	0.125	0.042	0.08	0.004	0.08
Gd	0.18	0.99	0.48	1.75	0.65	2.48	0.37	2.17	1.34	0.27	0.236	0.439	0.119	0.30	0.01	0.30
Tb	0.034	0.22	0.079	0.32	0.109	0.46	0.07	0.45	0.24	0.055	0.048	0.085	0.021	0.060	0.003	0.06
Dy	0.21	1.52	0.47	2.01	0.66	2.93	0.44	3.05	1.49	0.38	0.327	0.560	0.136	0.40	0.02	0.38
Ho	0.052	0.38	0.104	0.46	0.148	0.67	0.103	0.72	0.33	0.090	0.080	0.131	0.033	0.097	0.006	0.09
Er	0.16	1.19	0.29	1.30	0.41	1.92	0.30	2.07	0.95	0.27	0.236	0.379	0.105	0.29	0.01	0.28
Tm	0.025	0.18	0.044	0.19	0.061	0.28	0.045	0.305	0.137	0.041	0.037	0.058	0.017	0.044	0.002	0.05
Yb	0.16	1.21	0.28	1.19	0.39	1.67	0.30	1.91	0.84	0.27	0.242	0.364	0.119	0.28	0.01	
Lu	0.03	0.20	0.047	0.185	0.064	0.25	0.051	0.30	0.134	0.045	0.042	0.060	0.022	0.049	0.003	0.05
Hf	0.08	0.22	0.19	0.82	0.32	0.92	0.14	1.05	0.56	0.11	0.100	0.211	0.068	0.13	0.01	0.1
Ta	0.039	0.010	0.065	0.046	0.131	0.018	0.022	0.007	0.19	0.0058	0.0033	0.0039	0.022	0.018	0.0004	0.02
Pb	0.19	0.57	0.43	0.43	0.33	0.17	0.28	0.61	0.43	0.13	0.11	0.11	0.15	12.0	1.6	13
Th	0.27	1.29	0.31	0.97	0.27	0.27	0.23	1.36	0.52	0.038	0.012	0.03	0.05	0.074	0.018	0.07
U	0.063	0.27	0.084	0.18	0.076	0.07	0.092	0.46	0.156	0.018	0.007	0.015	0.010	0.051	0.009	0.07
Zr/Nb	3.9	45.7	4.6	32.2	4.6	25.6	8.9	977	7.3	31.1	37.1	40.3	11.3	68		80
Nb/La	0.143	0.006	0.28	0.038	0.75	0.10	0.083	0.001	0.18	0.43	0.50	0.30	0.53	0.17		0.14
Nb/Ta	21.3	21.3	24.2	19.4	20.7	59.2	23.4	5.6	18.1	25.1	32.2	52.4	16.5	2.9		2.5
Zr/Hf	40.6	43.7	38.7	35.3	39.7	29.6	32.6	36.2	44.3	39.5	39.1	39.2	60.7	28.1		40

Fs = feldspar, Ox = oxide, WR = whole rock, S.D. = standard deviation, R.V. = recommended value.
9513-7, -8, -13, -36 are metasomatised peridotites with abundant Ti-oxides and feldspar. 9512-5 is a cpx-poor lherzolite without feldspar and Ti-oxides; 9513-2, -4, -34 are cpx-rich lherzolites with no or very little feldspar and Ti-oxides.

If that value is disregarded, a low-weighted average (20.1) is obtained.

5. Composition of whole-rock peridotites and silicate minerals

Solution ICPMS analyses of whole-rock samples, cpx separates and a feldspar–cpx–ol–Ti-oxide metasomatic aggregate (Fig. 1b) are given in Table 3. The abundances of moderately incompatible heavy REE in the whole rocks and cpx are positively correlated with modal cpx, consistent with origin as residues of variable degrees of partial melting (Fig. 6 and unpublished data of D. Ionov). Similarly, two feldspar-free whole-rock samples show consistent depletion in medium REE and LREE (except for a La inflection) relative to heavy (H) REE on primitive mantle-normalised diagrams (Fig. 6). By comparison, all peridotites containing feldspar and Ti-rich oxides are enriched in light over heavy REE and have higher Nb and Ta (but not Ti, Zr and Hf) than the other xenoliths (Fig. 6).

Cpx from the feldspar–Ti-oxide-bearing xenoliths is enriched in light REE (Table 3) and has obviously been metasomatised. Yet, it is not clear whether it is chemically equilibrated with the Ti-oxide-bearing metasomatic materials because the latter occur as cross-cutting veins or fine-grained pockets and therefore do not appear to be in textural equilibrium with coarse-grained minerals of the host peridotite. We note, however, that the similarities between the REE patterns of whole rocks and cpxs on the one hand, and the positive correlation between enrichments in LREE and in Nb and Ta in the whole rocks on the other hand, argue for cpx enrichment in the same event that precipitated the Ti-oxides. The coarse cpx from the metasomatised xenoliths has much higher abundances of REE, Sr, Y, Th, U, Zr, Hf than the whole rocks but contains less Nb and Ta, resulting in extremely low Nb/La ratios (0.001–0.1; Table 3). This clearly indicates that a large proportion of Nb and Ta, unlike most other lithophile elements, resides elsewhere. No Nb was detected by EPMA in fine-grained cpx from the feldspar–Ti-oxide-rich pockets (Fig. 1b). Even if it has moderately elevated Nb abundances (below EPMA detection limit), the fine-grained cpx is not likely to be a significant host for Nb–Ta in the rock because its modal abundance is at least an order of magnitude lower than the coarse primary cpx.

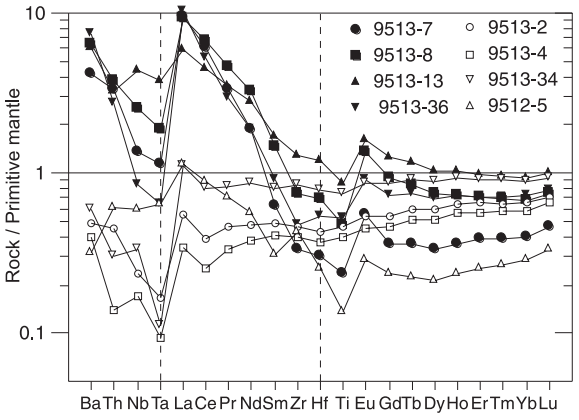

Fig. 6. Primitive mantle-normalised [1] trace element abundance patterns for whole-rock peridotites. Filled symbols are metasomatised peridotites with abundant Ti-oxides and feldspar; empty symbols are peridotites that contain no or very little feldspar or Ti-oxides.

Nb/Ta in most of the whole-rock peridotites is moderately superchondritic (21–25) (Table 3, Fig. 6). Two samples have yielded much higher Nb/Ta (32–52), but these values may be less precise because of very low Ta (≤ 4 ppb). Zr/Hf in most samples is mildly superchondritic (39–41), except in 9513-36 (33). Altogether, nearly all the Barhatny peridotites have generally similar Nb/Ta and Zr/Hf signatures. The only exception is sample 9512-5 with a near-chondritic Nb/Ta (16.5) and a very high Zr/Hf (61). Compared to the other xenoliths, 9512-5 is the only feldspar-free peridotite enriched in LREE and has the lowest modal cpx. All the xenoliths have subchondritic Nb/La ratios (0.08–0.75; $Nb/La_{ch} = 1.01$ [1,3]).

6. Discussion

6.1. Ti-oxide minerals as mineral hosts for trace elements in whole-rock peridotites

The residence of trace elements in mantle rocks

Table 4
Element abundances (in ppm), modal ratios and proportions of whole-rock Nb, Zr and Ti hosted in minerals of peridotites

Phase	Sample No.	% Nb in WR	% Zr in WR	% Ti in WR	Modal ratio	Ti	Zr	Nb	La	Ce	Yb	Hf	Ta	Sr
Cpx	9513-13	5	30	36	0.139	2630	27.1	1.06	10.4	19	1.67	0.92	0.018	184
Cpx	9513-7	2	27	26	0.091	752	9.5	0.208	32.8	60.4	1.21	0.217	0.010	354
Opx	9513-13	0.1	2	16	0.265	614	1.02	0.013	0.084	0.11	0.26	0.030	0.001	0.56
Opx	9513-7	0.5	2	15	0.205	186	0.390	0.022	0.134	0.26	0.17	0.009		0.61
Fs	9513-13	1.5	1	4	0.026	1473	3.2	1.64	25.5	23.8	0.4	0.068	0.078	861
Fs	9513-7	5			0.027									
Rutile	9513-13	91	17	5	0.0001	544 500	21 500	24 700						
Rutile	9513-7	93	33	14	0.00007	544 500	16 500	12 100						
Armalc	9513-13	2	51	8	0.0002	381 000	32 000	305	6848	9181		797	13.9	
Armalc	9513-7	1.4	39	6	0.00004		32 000							
Ilm	9513-13			33	0.001	332 000								
Ilm	9513-7			40	0.0012	332 000								

EPMA averages are given for Ti-oxides (Tables 1–3). Hf in armalcolite (Armalc) estimated assuming Zr/Hf = 47 (mean in Ti-oxides). Cpx and feldspar (Fs) values are from Table 3 (solution ICPMS). Orthopyroxene (Opx) values are from LAM-ICPMS analyses (unpublished data of D. Ionov).

is an important factor that must be taken into account in geochemical models. The behaviour of elements that largely reside in major minerals (pyroxenes, garnet and olivine) during melting and metasomatism can be approximated by modelling based on relatively well-defined peridotite phase diagrams and mineral/melt partition coefficients (K_D). However, melting relationships and K_D values of accessory phases are poorly known and may strongly depend on activities of volatiles and other minor components, which makes modeling in that case more complex and less precise (e.g. [31]).

Geochemical studies of spinel peridotites have found that only a small proportion of Nb and Ta of the bulk rocks resides in their major minerals. Amphibole and mica are major hosts for Nb and Ta in 'hydrous' mantle rocks [13,14,32], whereas various interstitial components have been invoked as hosts in 'anhydrous' peridotites. Ionov et al. [15] used mass-balance estimates to show that $< 10\%$ of Nb in spinel peridotites from SE Siberia reside in pyroxenes and olivine, compared to 70–80% of Zr, and argued that interstitial glass may be an important host for Nb and Ta. Eggins et al. [16] proposed a similar explanation for the Nb–Ta 'deficiency' in peridotites. Bodinier et al. [17] and Bedini and Bodinier [24] suggested that thin reaction layers coating spinel grains and composed of Ti-oxides and phlogopite are a predominant depository of Nb and Ta whereas silicate minerals account for 50–90% of Zr and Hf in whole rocks. Garrido et al. [33] suggested that Nb and Ta can also be hosted by inclusions in silicate minerals. Ionov et al. [20,34] and Gregoire et al. [27] argued that feldspar and Ti-oxides could be major hosts for incompatible elements in metasomatised feldspar-bearing peridotites from Hamar–Daban (Baikal region) and Kerguelen.

Here we use ICPMS and EPMA data on minerals and whole rocks combined with modal estimates for the xenoliths from Barhatny and laser ablation ICPMS analyses of orthopyroxene (unpublished data of D. Ionov) to provide quantitative estimates for the role of different minerals in the trace element budget of Ti-oxide-bearing peridotites (Table 4). We assume that trace element contributions of inclusion-free olivine and spinel

that have not been analysed in this work are insignificant in the whole rocks [15,16,24]. Consistent with the earlier studies, the share of cpx in the whole-rock budget of Nb and Ta is very low (1–5%) compared to $\geq$25–30% for Ti, Zr and Hf. A somewhat higher proportion of Nb and Ta estimated for cpx 9513-8 must be due to feldspar–Ti-oxide inclusions in that mineral separate as indicated by high Rb and Ba (Table 3) [33]. Assuming that rutile is a major carrier of Nb and Ta, we find that as little as 0.005–0.016% of rutile are sufficient to balance the Nb and Ta budget in the bulk rocks. These estimates are much lower than the maximal possible Ti-oxide contents in the peridotites deduced from 'excess' Ti in the bulk rocks (not hosted by the silicates and spinel). Other abundant Ti-rich oxides such as ilmenite ($\sim$55% TiO_2) may host the rest of the 'excess' Ti while loveringite may host Zr, Hf, La, Ce.

Fig. 7 illustrates the quantitative model we used to assess the budget of several elements in two whole-rock samples by successively adding estimated amounts of different Ti-oxides to the major minerals. Pyroxenes and feldspar account for nearly all Sr and Yb (HREE) in the bulk rocks but not for HFSE, La, Ce. We calculate step by step the amounts of (1) rutile necessary to account for the remaining Nb and Ta in the whole rock followed by (2) loveringite to account for the remaining Zr and Hf (or La and Ce, whatever comes first) and finally (3) ilmenite to balance Ti (assuming it contains no Zr and Nb). The resulting model estimates are given in Table 4. The model yields a close match for the whole-rock budget of all the HFSE and of La in 9513-13. The amount of loveringite required to balance La and Ce in 9513-7 would result in excess Zr and Hf in the bulk rock. However, the composition of the single loveringite grain analysed in that sample may not be representative in terms of (La,Ce)/(Zr,Hf) ratios.

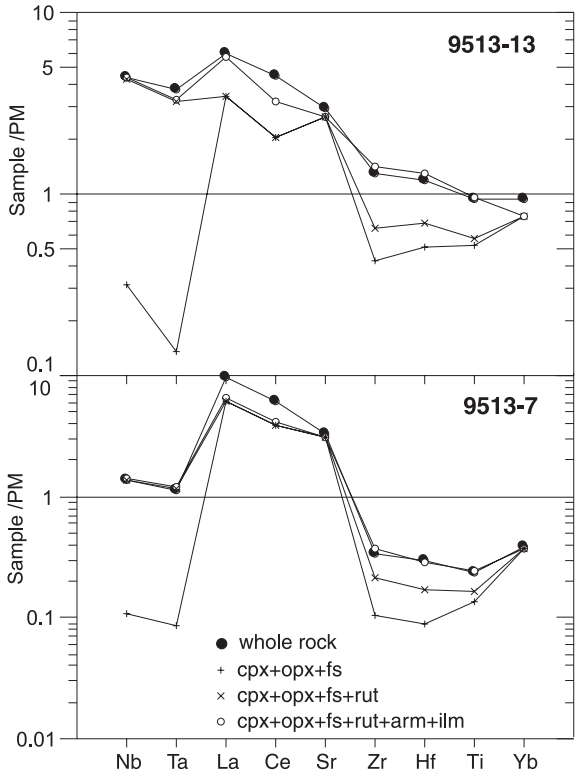

Fig. 7. A comparison of trace element patterns (primitive mantle-normalised after [1]) measured in whole rocks with estimates obtained from mineral compositions and modal abundances (see Table 4 and Section 6.1).

6.2. *The impact of Ti-oxide minerals on Nb/Ta and Zr/Hf in whole-rock peridotites*

The inference that most of Nb and Ta in the metasomatised peridotites from Barhatny reside in Ti-oxides also implies that those Nb–Ta-rich accessory minerals must control whole-rock Nb/Ta values. This is consistent with our data for two peridotites in which several Ti-oxides were analysed by high-precision EPM. The arithmetic mean Nb/Ta for rutile in sample 9513-7 (22.9) and abundance-weighted average (22.1) are within the analytical error (see Appendix of the **Background Data Set**[1]) of the whole-rock Nb/Ta obtained by solution ICPMS (21.3 $\pm$ 1.5). Similarly, mean Nb/Ta for Ti-oxides in 9513-13 (20.7) is identical to the measured whole-rock Nb/Ta. Thus, the whole-rock Nb/Ta of the metasomatised peridotites could be constrained from a representative number of analyses of accessory Ti-oxides.

Experimental work indicated that Nb/Ta in rutile may differ from that in coexisting melt or fluid [28,35]. However, results obtained on different

systems and at different conditions are not always consistent, and it remains unsure whether (and which way) rutile precipitation may fractionate Nb from Ta [36]. Furthermore, it is not clear whether the Barhatny peridotites were metasomatised under open- or closed-system conditions (i.e. batch crystallisation versus fluid percolation) and therefore whether the superchondritic Nb/Ta in the xenoliths are signatures of the initial metasomatic fluid or a consequence of Ti-oxide fractionation.

Zr and Hf are much more compatible in cpx than Nb and Ta, as illustrated by systematically higher Zr/Nb in cpx than in whole rocks (Table 3), and consistent with experimental data [36]. Pyroxenes appear to be predominant hosts for Zr and Hf in the shallow mantle [14,24,33]. In spite of the very high Zr and Hf found in some Ti-rich oxides, the whole-rock Zr/Hf in the Barhatny peridotites are also strongly affected by pyroxenes, which host $\geq 1/3$ of those elements in the bulk rocks. ICPMS analyses have yielded similar Zr/Hf values for whole-rock peridotites 9513-7 and 9513-13 (40–41) and their cpx separates (40–44), whereas average Zr/Hf in their Ti-oxides we measured (mostly rutile) are somewhat higher (45–49).

6.3. The role of Ti-oxide minerals in HFSE residence and behaviour in the mantle

A conclusion that whole-rock Nb/Ta of metasomatised peridotites could be constrained from analyses of accessory Ti-oxides may be directly relevant to only a small proportion of mantle rocks in which those minerals are large enough for microprobe analyses [20,27,34,37]. Nevertheless, results of this study may be of much broader significance for mantle geochemistry if the Ti-oxide micro-phases are essential components in nondescript grain boundary materials that are believed to host much of the highly incompatible elements in mantle rocks. Small Ti-oxides may be easily overlooked, and high-quality polished sections are essential for their identification. Earlier, Bodinier et al. [17] and Bedini and Bodinier [24] argued that very small amounts of titanates in spinel peridotites may host nearly all Nb and Ta yet remain undetectable by routine optical microscopy inspection. Bedini et al. [38] showed that metasomatic fluid percolation may create negative Nb–Ta anomalies if accessory minerals with high partition coefficient for Nb and Ta (e.g. rutile) are present in the percolation column. We demonstrate that as little as 40–200 ppm (Table 4) of rutile and armalcolite hosts $\geq 95\%$ of Nb and $> 65\%$ of Zr in some Barhatny xenoliths and largely control Nb/Ta and Zr/Hf in the whole rocks. The same may be true for other metasomatised mantle peridotites that contain fine-grained or opaque interstitial materials (and no significant amounts of amphibole or phlogopite). Furthermore, interstitial glass, an important host for Nb and Ta in some xenoliths [15,16], may have inherited part of its HFSE inventory from pre-existing Ti-oxides that melted during entrapment and transport of the xenoliths by host magma.

The data on the Barhatny xenoliths characterise inter-mineral and mineral/whole-rock trace element partitioning in common (except that they contain relatively large Ti-oxides) mantle peridotites and are complementary to experimental results on mineral/melt and mineral/fluid equilibria obtained on basaltic or synthetic systems. The much lower Nb and Zr found in ilmenite than in rutile in this work are consistent with experimental data [35]. By contrast, rutiles from Barhatny xenoliths are generally not enriched in Nb relative to Zr ($Zr/Nb \sim 1$), whereas experimental work yielded higher rutile/melt and rutile/fluid K_D for Nb and Ta than for Zr and Hf [28,36,39]. On the other hand, Zr/Nb in rutile from the xenoliths are strongly subchondritic ($Zr/Nb(ch) = 15.7$; [1]), implying that rutile preferentially incorporates Nb relative to Zr in the mantle. Rutile/cpx ratios for both Nb (23 000–58 000) and Zr (800–1700) in the Barhatny xenoliths are about two orders of magnitude higher than those from experimental work [36], although rutile/cpx equilibrium may be in question. The xenolith data also indicate that other Ti-oxides (e.g. loveringite, armalcolite), in addition to rutile, may be important hosts for HFSE (in particular Zr and Hf). Possible presence of Hf-rich accessory minerals should be assessed in Hf isotope studies of mantle rocks relying on analyses of cpx and garnet separates [40].

6.4. Nb/Ta and Zr/Hf in the Barhatny xenoliths in comparison with other mantle peridotites

A significant amount of data on Nb/Ta and Zr/Hf in mantle rocks and minerals has been recently obtained by solution ICPMS. Because of blank problems, poor counting statistics and other analytical problems at low Nb and Ta contents, in the discussion below we have discarded Nb/Ta values at Ta < 3 ppb unless good data quality has been demonstrated.

The only silicate minerals in the upper mantle that concentrate Nb and Ta are amphibole and phlogopite. These volatile-bearing minerals contain much less Nb and Ta than rutile but are by far more abundant and may account for a large proportion of their budget in the shallow off-cratonic lithospheric mantle [14]. Ionov and Hofmann [13] found a broad Nb/Ta range in a small number of mantle amphiboles and micas ranging from largely subchondritic in vein amphibole (11–20) to mostly superchondritic in amphibole and mica disseminated in peridotites (19–94) as well in the bulk rocks (12–70). Superchondritic Nb/Ta values were found in many peridotites possibly metasomatised by carbonatite-rich fluids/melts and/or containing silicate glass [41,42]. That may indicate that certain types of mantle metasomatism can impart specific Nb/Ta to mantle rocks, though some workers argued against such a link [43]. Experimental work has found that amphibole/melt K_D(Nb/Ta) may vary from 0.7 to 1.6 depending on its composition and thus amphibole precipitation may change Nb/Ta in the residual melt [44].

Selected literature Nb/Ta data on whole-rock peridotites [38,45–48] are plotted in Fig. 8 together with our results. Nb/Ta is mainly subchondritic (average 12) in abyssal peridotites from the East Pacific Rise and close to chondritic (average 17.4) in peridotite massifs (Ronda and Horoman). The abyssal and massif peridotites typically have subchondritic Zr/Hf (average 25) and La/Yb (Fig. 8). Those features are consistent with an origin as partial melting residues. Because cpx/melt partition coefficients are lower for Nb than for Ta,

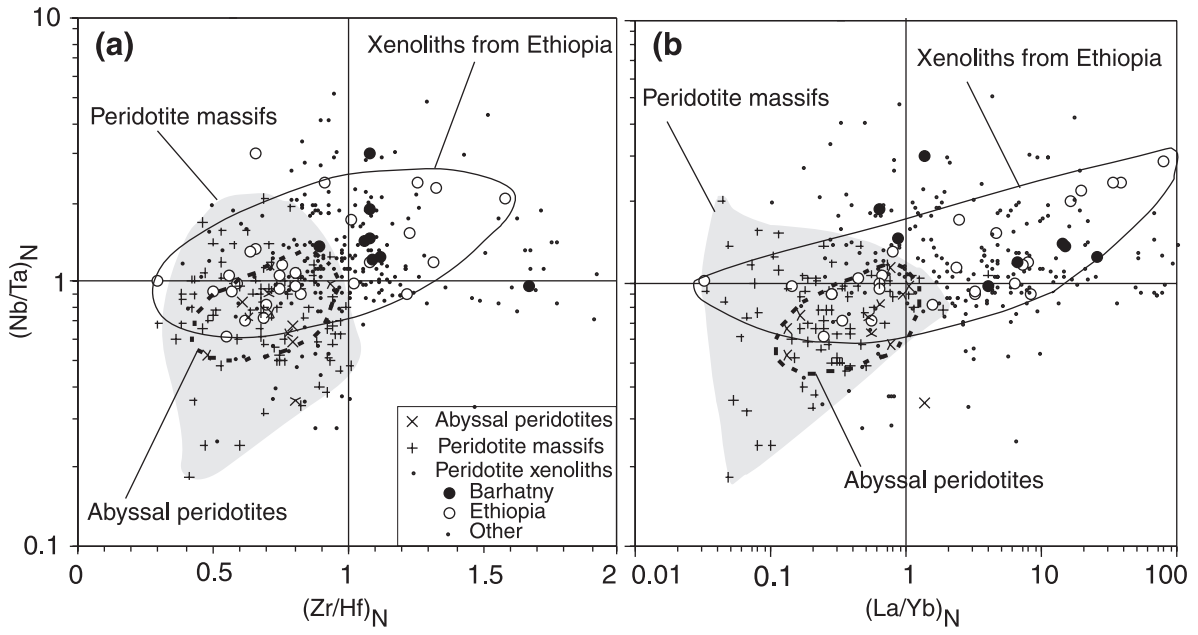

Fig. 8. Nb/Ta in mantle peridotites from this work in comparison with literature data plotted versus Zr/Hf (a) and La/Yb (b). Data sources: Ethiopia [38]; French Massif Central ([45] and unpublished data of O. Alard, X. Lenoir, J.-M Dautria, J.-L. Bodinier); Kaapvaal and Hoggar (F. Kalfoun); East Pacific Rise (unpublished data of M. Godard and Hékinian); Ronda ([46,47] and unpublished data of J.-L. Bodinier and M. Remaidi); Horoman [48].

and $K_D(Zr) < K_D(Hf)$ [10,11,49], shallow partial melting of primitive mantle must produce residues with lower Nb/Ta and Zr/Hf, and melts with higher Nb/Ta and Zr/Hf. $(Nb/Ta)_N < 1$ ($_N$ denotes values normalised to primitive mantle) were recently obtained also for massif peridotites from northern Italy [50] by MC-ICPMS.

Peridotite xenoliths in volcanic rocks show a broad range of Nb/Ta variation, but $(Nb/Ta)_N > 1$ and $(La/Yb)_N > 1$ appear to be more common (mean $(Nb/Ta)_N = 24$). An important factor in the data scatter in Fig. 8 is low accuracy of Nb/Ta values at low Ta. Remarkably, when analyses with < 7 ppb Ta and a single sample with anomalously high Zr and Nb are discarded, peridotites from Ethiopia [38] show a rough positive correlation of Nb/Ta with La/Yb ($R^2 = 0.75$), which indicates an increase in Nb/Ta with increasing degrees of metasomatism. Downes [51] noted that mantle xenoliths from Europe are more commonly enriched in LREE than massif peridotites. The dominant $(La/Yb)_N > 1$ in the xenoliths are consistent with a commonly held view that lithospheric mantle has suffered widespread metasomatism (e.g. [2]). Fig. 8 indicates that $(Nb/Ta)_N > 1$ may be typical for metasomatised mantle, and that continental lithospheric mantle may have a superchondritic mean Nb/Ta. If the latter is true, the lithospheric mantle may provide a reservoir complementary to those of depleted MORB-type mantle and continental crust, both of which have $(Nb/Ta)_N < 1$ [5–7]. However, the lithospheric mantle is not likely to counterbalance the subchondritic reservoirs in the bulk earth because of a much higher mass of the asthenospheric mantle and higher Nb and Ta in the crust. Furthermore, all samples in this study as well as many other metasomatised peridotite xenoliths have negative Nb–Ta anomalies on PM-normalised distribution diagrams (Fig. 6), i.e. subchondritic Nb/La (Table 3). By contrast, a reservoir complementary to the depleted mantle and continental crust must have superchondritic Nb/La in addition to superchondritic Nb/Ta [5,9]. Broad Nb/La variations in mantle peridotites (in addition to significant scatter of the Nb/Ta values, Fig. 8) make it difficult to demonstrate whether the lithospheric mantle has on average superchondritic Nb/La and Nb/Ta and thus is indeed complementary to the depleted mantle.

7. Conclusions

High-precision EPMA can be used to reliably determine HFSE and LREE at > 200 ppm in accessory minerals and to estimate Nb/Ta and Zr/Hf with ± 2–6% accuracy at Ta and Hf ≥ 1000 ppm. Whole-rock Nb/Ta in peridotites can be assessed from EPM analyses of representative numbers of (Nb,Ta)-rich phases. Mass balance calculations indicate that only 1–5% of Nb and Ta in some metasomatised off-cratonic peridotites reside in major minerals and that as little as 0.005–0.02% of modal rutile may account for the Nb–Ta budget of the rocks. By contrast, $\geq 1/3$ of Zr and Hf are hosted by the major minerals. Ca-bearing Ti-oxides may contain a significant proportion of Zr, Hf, La and Ce in the bulk peridotites. The Ti-rich oxide micro-phases may be important components of nondescript grain boundary materials, whose mineralogical composition cannot be defined optically or by EPMA, and which are inferred to host much of highly incompatible trace elements in mantle rocks [33].

Most of the Barhatny peridotites have superchondritic Nb/Ta. Literature data indicate that $(Nb/Ta)_N > 1$ may be a common feature of metasomatised mantle peridotites and of continental lithospheric mantle in general. By contrast, unmetasomatised abyssal and massif peridotites commonly have subchondritic Nb/Ta and Zr/Hf consistent with partial melting relationships not obscured by subsequent metasomatism.

Acknowledgements

D.I. thanks V. Prikhod'ko for guidance in fieldwork and donating some samples used in this study and E. Essene for advice on Ti-oxide classification. S. Pourtales and O. Bruguier provided technical assistance during ICPMS analyses. J.-L. Bodinier and M. Godard made available some unpublished trace element analyses. Reviews by M. Barth and an anonymous reviewer and com-

ments by J.-L. Bodinier, J. Scoates and D. Weis helped to improve the paper. D.I. acknowledges DRI post-doctoral fellowships from Université Libre de Bruxelles and FNRS.*[BOYLE]*

References

[1] A.W. Hofmann, Chemical differentiation of the Earth: the relationship between mantle, continental crust, and oceanic crust, Earth Planet. Sci. Lett. 90 (1988) 297–314.
[2] W.F. McDonough, Constraints on the composition of the continental lithospheric mantle, Earth Planet. Sci. Lett. 101 (1990) 1–18.
[3] W.F. McDonough, Partial melting of subducted oceanic crust and isolation of its residual eclogitic lithology, Phil. Trans. R. Soc. London Ser. A 335 (1991) 407–418.
[4] K.P. Jochum, J. Stolz, High-precision Nb, Ta, Zr, and Y data for carbonaceous chondrites: constraints on solar system Nb/Ta and Zr/Nb ratios, Meteorit. Planet. Sci. 32 (1997) 67.
[5] M.G. Barth, W.F. McDonough, R.L. Rudnick, Tracking the budget of Nb and Ta in the continental crust, Chem. Geol. 165 (2000) 197–213.
[6] T. Plank, C.H. Langmuir, The chemical composition of subducting sediment and its consequences for the crust and mantle, Chem. Geol. 145 (1998) 325–394.
[7] K.P. Jochum, A.W. Hofmann, Nb/Ta in MORB and continental crust implications for a superchondritic Nb/Ta reservoir in the mantle, EOS 79 (1998) 354.
[8] B.S. Kamber, K.D. Collerson, Role of 'hidden' deeply subducted slabs in mantle depletion, Chem. Geol. 166 (2000) 241–254.
[9] R.L. Rudnick, M. Barth, I. Horn, W.F. McDonough, Rutile-bearing refractory eclogites missing link between continents and depleted mantle, Science 287 (2000) 278–281.
[10] C.C. Lundstrom, H.F. Shaw, F.J. Ryerson, Q. Williams, J. Gill, Crystal chemical control of cpx-melt partitioning in the Di-Ab-An system: implications for elemental fractionations in the depleted mantle, Geochim. Cosmochim. Acta 62 (1998) 2849–2862.
[11] T.H. Green, Significance of Nb/Ta as an indicator of geochemical processes in the crust-mantle system, Chem. Geol. 120 (1995) 347–359.
[12] C. Dupuy, J.M. Liotard, J. Dostal, Zr/Hf fractionation in intraplate basaltic rocks: carbonate metasomatism in the mantle source, Geochim. Cosmochim. Acta 56 (1992) 2417–2423.
[13] D.A. Ionov, A.W. Hofmann, Nb-Ta-rich mantle amphiboles and micas: implications for subduction-related metasomatic trace element fractionations, Earth Planet. Sci. Lett. 131 (1995) 341–356.
[14] D.A. Ionov, S.Y. O'Reilly, W.L. Griffin, Volatile-bearing minerals and lithophile trace elements in the upper mantle, Chem. Geol. 141 (1997) 153–184.
[15] D.A. Ionov, V.S. Prikhod'ko, S.Y. O'Reilly, Peridotite xenoliths from the Sikhote-Alin, south-eastern Siberia, Russia: trace element signatures of mantle beneath a convergent continental margin, Chem. Geol. 120 (1995) 275–294.
[16] S.M. Eggins, R.L. Rudnick, W.F. McDonough, The composition of peridotites and their minerals: a laser ablation ICP-MS study, Earth Planet. Sci. Lett. 154 (1998) 53–71.
[17] J.-L. Bodinier, C. Merlet, R.M. Bedini, F. Simien, M. Remaidi, C.J. Garrido, Distribution of niobium, tantalum, and other highly incompatible trace elements in the lithospheric mantle: the spinel paradox, Geochim. Cosmochim. Acta 60 (1996) 545–550.
[18] F.J. Ryerson, E.B. Watson, Rutile saturation in magmas: implications for Ti-Nb-Ta depletion in island-arc basalts, Earth Planet. Sci. Lett. 86 (1987) 225–239.
[19] S.E. Haggerty, Oxide mineralogy of the upper mantle, in: D.H. Lindsley (Ed.), Oxide Minerals: Petrologic and Magnetic Significance, Mineralogical Society of America, Washington, DC, 1991, pp. 355–416.
[20] D.A. Ionov, M. Grégoire, V.S. Prikhod'ko, Feldspar-Ti-oxide metasomatism in off-cratonic continental and oceanic upper mantle, Earth Planet. Sci. Lett. 165 (1999) 37–44.
[21] C. Merlet, J.-L. Bodinier, Electron microprobe determination of minor and trace transition elements in silicate minerals: A method and its application to mineral zoning in the peridotite nodule PHN1611, Chem. Geol. 83 (1990) 55–69.
[22] D.A. Ionov, L. Savoyant, C. Dupuy, Application of the ICP-MS technique to trace element analysis of peridotites and their minerals, Geostand. Newsl. 16 (1992) 311–315.
[23] M. Godard, D. Jousselin, J.-L. Bodinier, Relationships between geochemistry and structure beneath a palaeospreading centre: a study of the mantle section in the Oman ophiolite, Earth Planet. Sci. Lett. 180 (2000) 133–148.
[24] R.M. Bedini, J.-L. Bodinier, Distribution of incompatible trace elements between the constituents of spinel peridotite xenoliths: ICP-MS data from the East African rift, Geochim. Cosmochim. Acta 63 (1999) 3883–3900.
[25] D.A. Ionov, Mantle metasomatism by fluids with low water activity: feldspar-Ti-oxide-bearing peridotite xenoliths in basalts from SE Siberia, J. Conf. Abstr. 4 (1999) 364–365.
[26] L. Wang, E. Essene, Y. Zhang, Mineral inclusions in pyrope crystals from Garnet Ridge, Arizona, USA: implications for processes in the upper mantle, Contrib. Mineral. Petrol. 135 (1999) 164–178.
[27] M. Grégoire, J.-P. Lorand, S.Y. O'Reilly, J.-Y. Cottin, Armalcolite-bearing, Ti-rich metasomatic assemblages in harzburgite xenoliths from the Kerguelen Islands: implications for the oceanic mantle budget of high-field strength elements, Geochim. Cosmochim. Acta 64 (2000) 673–694.
[28] J.M. Brenan, H.F. Shaw, D.L. Phinney, F.J. Ryerson, Rutile-aqueous fluid partitioning of Nb, Ta, Hf, Zr,

U and Th: implications for high field strength element depletions in island-arc basalts, Earth Planet. Sci. Lett. 128 (1994) 327–339.
[29] J.F.W. Bowles, Definition and range of naturally occurring minerals with pseudobrookite structure, Am. Mineral. 73 (1988) 1377–1383.
[30] T.H. Green, N.J. Pearson, High-pressure, synthetic loveringite-davidite and its rare earth element geochemistry, Mineral. Mag. 51 (1987) 145–149.
[31] S. Foley, Vein-plus-wall-rock melting mechanisms in the lithosphere and the origin of potassic alkaline magmas, Lithos 28 (1992) 435–453.
[32] M. Tiepolo, P. Bottazzi, S. Foley, R. Oberti, R. Vannucci, A. Zanetti, Fractionation of Nb and Ta from Zr and Hf at mantle depths: the role of titanian pargasite and kaersutite, J. Petrol. 42 (2001) 221–232.
[33] C.J. Garrido, J.-L. Bodinier, O. Alard, Incompatible trace element partitioning and residence in anhydrous spinel peridotites and websterites from the Ronda orogenic peridotite, Earth Planet. Sci. Lett. 181 (2000) 341–358.
[34] D.A. Ionov, S.Y. O'Reilly, I.V. Ashchepkov, Feldspar-bearing lherzolite xenoliths in alkali basalts from Hamar-Daban, southern Baikal region, Russia, Contrib. Mineral. Petrol. 122 (1995) 174–190.
[35] T.H. Green, N.J. Pearson, An experimental study of Nb and Ta partitioning between Ti-rich minerals and silicate liquids at high pressure and temperature, Geochim. Cosmochim. Acta 51 (1987) 55–62.
[36] R. Stalder, S.F. Foley, G.P. Brey, I. Horn, Mineral-aqueous fluid partitioning of trace elements at 900–1200 degrees C and 3.0 Gpa: new experimental data for garnet, cpx and rutile and implications for mantle metasomatism, Geochim. Cosmochim. Acta 62 (1998) 1781–1801.
[37] F. Chalot-Prat, M. Arnold, Immiscibility between calcio-carbonatitic and silicate melts and related wall rock reactions in the upper mantle a natural case study from Romanian mantle xenoliths, Lithos 46 (1999) 627–659.
[38] R.M. Bedini, J.-L. Bodinier, J.-M. Dautria, L. Morten, Evolution of LILE-enriched small melt fractions in the lithospheric mantle: a case study from the East African Rift, Earth Planet. Sci. Lett. 153 (1997) 67–83.
[39] S.F. Foley, M.G. Barth, G.A. Jenner, Rutile/melt partition coefficients for trace elements and an assessment of the influence of rutile on the trace element characteristics of subduction zone magmas, Geochim. Cosmochim. Acta 64 (2000) 933–938.
[40] J. Blichert-Toft, D.A. Ionov, F. Albarède, The nature of the sub-continental lithospheric mantle: Hf isotope evidence from garnet peridotite xenoliths from Siberia, J. Conf. Abstr. 5 (2000) 217.
[41] D.A. Ionov, C. Dupuy, S.Y. O'Reilly, M.G. Kopylova, Y.S. Genshaft, Carbonated peridotite xenoliths from Spitsbergen: implications for trace element signature of mantle carbonate metasomatism, Earth Planet. Sci. Lett. 119 (1993) 283–297.
[42] D.A. Ionov, A.W. Hofmann, N. Shimizu, Metasomatism-induced melting in mantle xenoliths from Mongolia, J. Petrol. 35 (1994) 753–785.
[43] A. Laurora, M. Mazzucchelli, G. Rivalenti, R. Vannucci, A. Zanetti, M.A. Barbieri, C.A. Cingolani, Metasomatism and melting in carbonated peridotite xenoliths from the mantle wedge: the Gobernador Gregores case (southern Patagonia), J. Petrol. 42 (2001) 69–87.
[44] M. Tiepolo, R. Vannucci, R. Oberti, S. Foley, P. Bottazzi, A. Zanetti, Nb and Ta incorporation and fractionation in titanian pargasite and kaersutite: crystal-chemical constraints and implications for natural systems, Earth Planet. Sci. Lett. 176 (2000) 185–201.
[45] X. Lenoir, C.J. Garrido, J.-L. Bodinier, J.-M. Dautria, Contrasting lithospheric mantle domains beneath the Massif Central (France) revealed by geochemistry of peridotite xenoliths, Earth Planet. Sci. Lett. 181 (2000) 359–375.
[46] X. Lenoir, C.J. Garrido, J.-L. Bodinier, J.-M. Dautria, F. Gervilla, The recrystallisation front of the Ronda peridotite: Evidence for melting and thermal erosion of subcontinental lithospheric mantle beneath the Alboran basin, J. Petrol. 42 (2001) 141–158.
[47] D. Van der Wal, J.-L. Bodinier, Origin of the recrystallisation front in the Ronda peridotite by km-scale pervasive porous melt flow, Contrib. Mineral. Petrol. 122 (1996) 387–405.
[48] E. Takazawa, F.A. Frey, N. Shimizu, M. Obata, Whole rock compositional variations in an upper mantle peridotite (Horoman, Hokkaido, Japan): are they consistent with a partial melting process, Geochim. Cosmochim. Acta 64 (2000) 695–716.
[49] T. Skulski, W. Minarik, E.B. Watson, High-pressure experimental trace-element partitioning between cpx and basaltic melts, Chem. Geol. 117 (1994) 127–147.
[50] C. Münker, S. Weyer, G. Wörner, K. Mezger, The behaviour of HFSE in subduction zones: new insights from Hf isotopes and high precision measurements of Nb/Ta, Zr/Hf and Lu/Hf in arc rocks from Kamchatka, J. Conf. Abstr. 6 (2001) 384.
[51] H. Downes, Formation and modification of the shallow sub-continental lithospheric mantle: a review of geochemical evidence from ultramafic xenolith suites and tectonically emplaced ultramafic massifs of western and central Europe, J. Petrol. 42 (2001) 233–250.